

Double-step truncation procedure for large-scale shell-model calculations

L. Coraggio,¹ A. Gargano,¹ and N. Itaco^{1,2}

¹*Istituto Nazionale di Fisica Nucleare,
Complesso Universitario di Monte S. Angelo, Via Cintia - I-80126 Napoli, Italy*

²*Dipartimento di Matematica e Fisica, Seconda Università di Napoli,
viale Abramo Lincoln 5 - I-81100 Caserta, Italy*

We present a procedure that is helpful to reduce the computational complexity of large-scale shell-model calculations, by preserving as much as possible the role of the rejected degrees of freedom in an effective approach. Our truncation is driven first by the analysis of the effective single-particle energies of the original large-scale shell-model hamiltonian, so to locate the relevant degrees of freedom to describe a class of isotopes or isotones, namely the single-particle orbitals that will constitute a new truncated model space. The second step is to perform an unitary transformation of the original hamiltonian from its model space into the truncated one. This transformation generates a new shell-model hamiltonian, defined in a smaller model space, that retains effectively the role of the excluded single-particle orbitals. As an application of this procedure, we have chosen a realistic shell-model hamiltonian defined in a large model space, set up by seven and five proton and neutron single-particle orbitals outside ⁸⁸Sr, respectively. We study the dependence of shell-model results upon different truncations of the original model space for the Zr, Mo, Ru, Pd, Cd, and Sn isotopic chains, showing the reliability of this truncation procedure.

PACS numbers: 21.60.Cs, 21.30.Fe, 23.20.Lv, 27.60.+j

I. INTRODUCTION

Large-scale shell-model (LSSM) calculations have become a well-established approach to obtain a microscopic theoretical description of the collective properties of atomic nuclei. This goal has been evident since the early papers where the rotational motion of some *pf*-shell nuclei [1] or the large γ -softness of ⁶⁴Ge [2], already observed in experimental studies, were described in terms of the shell model (SM) instead of resorting to nuclear collective models.

In present days, powerful computing devices are widely accessible and make more feasible to approach SM calculations with large model spaces for nuclei with many valence nucleons. This has given the opportunity to many nuclear-theory groups to study exotic features of the atomic nuclei within a microscopic approach, so supporting the experimental efforts to enlarge the knowledge of the chart of the nuclides in the rare-ion-beam era. In recent years, it is worth mentioning the study of the onset of collectivity in some isotopic and isotonic chains [3–6], the revelation of novel collective features [7–10] and of the island-of-inversion phenomenon [11], the description of the shell evolution in many heavy-mass nuclei [12–15]. Along with these SM studies, it should be also pointed out that a notable theoretical effort has been devoted to enhance the computational abilities of LSSM calculations [16–21].

In spite of the progress in solving eigenproblems of large complexity, there exists always a limit to the maximum dimension of matrices that can be diagonalized when solving the Schrödinger equation. This affects mostly the shell-model studies of heavy-mass nuclei, where the required model spaces own a large capacity, making the calculations for nuclei with many valence

nucleons very demanding.

For example, in Ref. [22] experimental data for light tin isotopes are compared with the results of LSSM calculations performed by considering ⁹⁰Zr as a closed core, and using the ANTOINE shell-model code [23]. Since the model space was made up by the six *sdgh* proton orbitals and the five neutron ones (excluding the *0g_{9/2}* orbital), exact calculations were not feasible, and the SM basis was truncated allowing up to $4p - 4h$ $Z = 50$ cross-shell excitations only.

A more recent example, which may be mentioned, is the observation of the onset of collectivity at $N = 40$ in the chromium and iron isotopic chains [6]. The latter has been interpreted as due to the interplay between the quadrupole-quadrupole component of the residual interaction and the central field in the sub-space spanned by the lowest $\Delta j=2$ orbitals of a major shell [24]. This interpretation is based on a LSSM calculation, where the model space is composed by the four *fp* proton orbitals and five *fpgd* neutron ones, with 4 and 6 valence protons and up to 12 valence neutrons. Also in this calculation, the diagonalization of the full SM basis, using the NATHAN code [25], was not feasible, and a truncation up to $14p - 14h$ excitations across the $Z = 28$ and $N = 40$ shell-closures was employed.

From the above examples, it is evident that computational difficulties, when dealing with large model spaces, arise evolving the number of the valence protons Z_{val} (isotonic chains) and/or of the valence neutrons N_{val} (isotopic chains), a typical situation for nuclei exhibiting exotic features.

The increase of the valence particles, however, comes along with the evolution of the theoretical effective single-particle energies (ESPE) for a given SM hamiltonian. Therefore, the behavior of the ESPE as a function of

the number of valence protons or neutrons may help to identify the relevant degrees of freedom to describe the spectroscopic characteristics of a certain nucleus.

In the present work, we propose a method, that we have already experienced in Ref. [26], which locates a very effective truncation of the model space, through the study of the ESPE of a SM hamiltonian H as a function of Z_{val} and/or N_{val} . Successively, we build up a new SM hamiltonian \tilde{H} defined in a reduced model space with a smaller number of orbitals, by way of an unitary transformation of the “mother hamiltonian” H .

As a testing ground, we consider the study of the quadrupole collectivity due to $Z = 50$ cross-shell excitations in even-even isotopic chains above ^{88}Sr .

First, we derive an effective shell-model hamiltonian starting from the CD-Bonn potential [27], whose high-momentum repulsive components are smoothed out using the $V_{\text{low-k}}$ approach [28], by way of the time-dependent perturbation theory [29, 30]. This will be done within a large model space, that includes seven *psdgh* proton orbitals and five *sdgh* neutron ones.

Then, we calculate and study the behavior of the proton and neutron ESPE as a function of the number of valence neutrons and protons. The analysis of the ESPE drives the choice to reduce the number of proton and neutron orbitals. Consequently, new effective hamiltonians defined in reduced model spaces and tailored to study certain isotopic chains, are derived by way of a unitary transformation of the starting shell-model hamiltonian. Finally, we perform SM calculations with these effective hamiltonians and compare the theoretical results so to quantify the reliability of this double-step procedure.

In the next section, we sketch out a few details about the derivation of our shell-model hamiltonians and effective charges of the electric quadrupole operators. We also present the results of the behavior of the calculated ESPE as a function of the valence protons. Besides this, we will discuss how we have derived the new effective hamiltonians, within two new truncated model spaces. In Section III, we present the results of our calculations for Zr, Mo, Ru, Pd, Cd, and Sn isotopes, comparing the results obtained with three different model spaces. In the last section a summary of the present work and an outlook of our future programs are reported. In Ref. [31] they can be found the calculated two-body matrix elements (TBME) of the effective shell-model interactions in the truncated model spaces.

II. OUTLINE OF CALCULATIONS

Our starting effective shell-model hamiltonian has been derived within the framework of the many-body perturbation theory, as mentioned in the Introduction, from the CD-Bonn NN potential [27]. More explicitly, first the high-momentum repulsive components of the bare NN potential have been renormalized by way of the so-called $V_{\text{low-k}}$ approach [28, 32], which provides a smooth

potential preserving exactly the onshell properties of the original NN potential up to a cutoff momentum $\Lambda = 2.6 \text{ fm}^{-1}$. Next, we have derived the shell-model hamiltonian using the well-known \hat{Q} -box plus folded-diagram method [30], where the \hat{Q} -box is a collection of irreducible valence-linked Goldstone diagrams which we have calculated through third order in the $V_{\text{low-k}}$ [33].

The effective hamiltonian H_{eff} can be written in an operator form as

$$H_{\text{eff}} = \hat{Q} - \hat{Q}' \int \hat{Q} + \hat{Q}' \int \hat{Q} \int \hat{Q} - \hat{Q}' \int \hat{Q} \int \hat{Q} \int \hat{Q} + \dots, \quad (1)$$

where the integral sign represents a generalized folding operation, and \hat{Q}' is obtained from \hat{Q} by removing terms of first order in $V_{\text{low-k}}$. The folded-diagram series is summed up to all orders using the Lee-Suzuki iteration method [34].

TABLE I: Theoretical shell-model SP energy spacings (in MeV) employed in present work (see text for details).

nlj	proton SP energies	neutron SP energies
$1p_{1/2}$	0.0	
$0g_{9/2}$	1.5	
$0g_{7/2}$	5.7	1.5
$1d_{5/2}$	6.4	0.0
$1d_{3/2}$	8.8	3.4
$2s_{1/2}$	8.7	2.2
$0h_{11/2}$	10.2	5.1

TABLE II: Proton and neutron effective charges of the electric quadrupole operator $E2$.

$n_a l_a j_a$	$n_b l_b j_b$	$\langle a e_p b \rangle$	$\langle a e_n b \rangle$
$0g_{9/2}$	$0g_{9/2}$	1.53	
$0g_{9/2}$	$0g_{7/2}$	1.58	
$0g_{9/2}$	$1d_{5/2}$	1.51	
$0g_{7/2}$	$0g_{9/2}$	1.77	
$0g_{7/2}$	$0g_{7/2}$	1.84	1.00
$0g_{7/2}$	$1d_{5/2}$	1.84	0.98
$0g_{7/2}$	$1d_{3/2}$	1.86	0.98
$1d_{5/2}$	$0g_{9/2}$	1.59	
$1d_{5/2}$	$0g_{5/2}$	1.73	0.92
$1d_{5/2}$	$1d_{5/2}$	1.73	0.87
$1d_{5/2}$	$1d_{3/2}$	1.71	0.90
$1d_{5/2}$	$2s_{1/2}$	1.76	0.73
$1d_{3/2}$	$0g_{7/2}$	1.83	0.94
$1d_{3/2}$	$1d_{5/2}$	1.79	0.93
$1d_{3/2}$	$1d_{3/2}$	1.81	0.92
$1d_{3/2}$	$2s_{1/2}$	1.83	0.75
$2s_{1/2}$	$1d_{5/2}$	1.73	0.73
$2s_{1/2}$	$1d_{3/2}$	1.73	0.73
$0h_{11/2}$	$0h_{11/2}$	1.89	0.87

From the effective hamiltonian both single-particle (SP) energies and two-body matrix elements of the residual interaction have been obtained [33], and we have

derived consistently the effective charges of the electric quadrupole operators at the same perturbative order.

The model space we have employed is spanned by the seven $1p_{1/2}$, $0g_{9/2}$, $0g_{7/2}$, $1d_{5/2}$, $1d_{3/2}$, $2s_{1/2}$, $0h_{11/2}$ proton orbitals and by the five $0g_{7/2}$, $1d_{5/2}$, $1d_{3/2}$, $2s_{1/2}$, $0h_{11/2}$ neutron orbitals, considering ^{88}Sr as an inert core. From now on, we will indicate this model space as [75], and consequently, we have dubbed the effective hamiltonian H^{75} , the superscript indicating the number of proton (seven) and neutron (five) model-space orbitals.

Such a large model space has been introduced so as to take explicitly into account the $Z = 50$ cross-shell excitations of protons jumping from the $1p_{1/2}$, $0g_{9/2}$ orbitals into the $sdgh$ ones.

In Table I the calculated single-particle energies are reported, and in Table II are reported theoretical proton and neutron effective charges, which are close to the usual empirical values ($e_p^{\text{emp}} = 1.5e$, $e_n^{\text{emp}} = 0.5 \div 0.8e$).

As previously mentioned, the major difficulty with H^{75} is the increasing computational complexity, when evolving the atomic number Z of the isotopic chain under investigation. In particular, if one focuses his attention on the tin chain - as we did in Ref. [26] - this hamiltonian cannot be diagonalized for any tin isotope with up-to-date shell-model codes.

It is then mandatory to find the way to reduce the dimensions of the matrices to be diagonalized, and consequently make the shell-model calculation feasible.

Here we present an approach, adopted for the first time in Ref. [26], which leads to new effective hamiltonians defined in truncated model spaces, by way of a unitary transformation of H^{75} . The choice of the truncation of the model space is driven by the behavior, as a function of Z_{val} and N_{val} , of the proton and neutron effective single-particle energies (ESPE) of the original hamiltonian H^{75} , so as to find out what are the most relevant degrees of freedom to describe the physics of nuclear systems of interest. To this end, we report in Figs. 1 and 2 the evolution of both proton and neutron ESPE as a function of Z_{val} . From the inspection of Fig. 1, it can be observed that an almost constant energy gap provides a separation between the subspace spanned by the $1p_{1/2}$, $0g_{9/2}$, $1d_{5/2}$, $0g_{7/2}$ proton orbitals and that spanned by the $2s_{1/2}$, $1d_{3/2}$, $0h_{11/2}$ ones. This leads to the conclusion that a reasonable truncation is to consider only the lowest four orbitals, as proton model space.

On the neutron side, Fig. 2 evidences that the filling of the proton $0g_{9/2}$ orbital induces a relevant energy gap at $Z = 50$ between the $1d_{5/2}$, $0g_{7/2}$ subspace and that spanned by the $2s_{1/2}$, $1d_{3/2}$, $0h_{11/2}$ orbitals. This gap, around 2.4 MeV, traces back to the tensor component of the proton-neutron interaction that is mainly responsible for the shell evolution [35].

On the above grounds, it looks reasonable that a neutron model space spanned only by the $1d_{5/2}$, $0g_{7/2}$ orbitals may provide the relevant features of the physics of isotopic chains with higher Z , such as Pd, Cd, and Sn

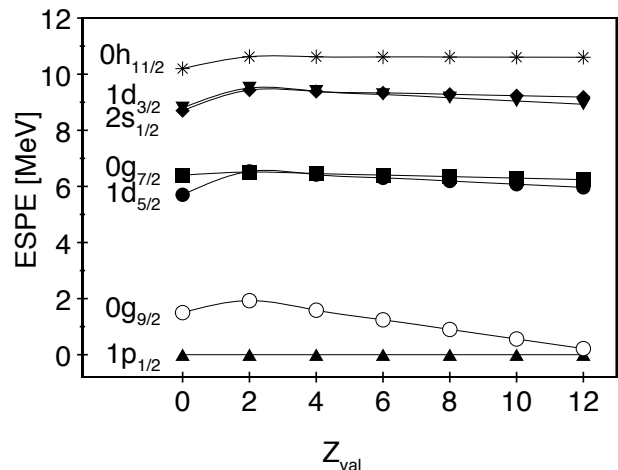


FIG. 1: Calculated proton effective single-particle energies of H^{75} as a function of the number of valence protons Z_{val} .

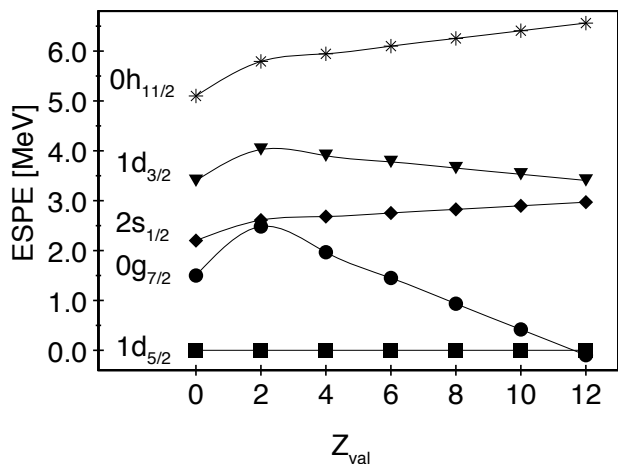


FIG. 2: Calculated neutron effective single-particle energies of H^{75} as a function of the number of valence protons Z_{val} .

isotopes.

Consequently, we have derived two new effective hamiltonians H_{eff}^{45} , H_{eff}^{42} , defined within two model spaces [45], [42] spanned by the $1p_{1/2}$, $0g_{9/2}$, $1d_{5/2}$, $0g_{7/2}$ proton orbitals, and by the $0g_{7/2}$, $1d_{5/2}$, $1d_{3/2}$, $2s_{1/2}$, $0h_{11/2}$ and $0g_{7/2}$, $1d_{5/2}$ neutron orbitals, respectively.

Here, we present a few details about the derivation of these effective hamiltonians, dubbed H_{eff}^{pn} , starting from the “mother hamiltonian” H^{75} .

The eigenvalue problem for H^{75} written in terms of its eigenvalues E_i and eigenfunctions ψ_i is the following:

$$H^{75}|\psi_i\rangle = E_i|\psi_i\rangle \quad , \quad (2)$$

where H^{75} may be partitioned as the sum of a single-particle hamiltonian H_0 and a residual two-body poten-

tial V :

$$H^{75} = H_0 + V \quad . \quad (3)$$

As it has been mentioned before, the analysis of the behavior of the ESPE induces a possible reduction of the number SP orbitals that span the model space. The original model space [75] is then splitted up in two subspaces $P \equiv P^{pn}$ and $Q \equiv Q^{7-p,5-n}$, with the projector P that can be expressed in terms of the H_0 eigenvectors

$$P = \sum_{i=1,d} |i\rangle\langle i| \quad H_0|i\rangle = E_i^0|i\rangle \quad . \quad (4)$$

We can define the P -space effective hamiltonian H_{eff}^{pn} by writing

$$H_{\text{eff}}^{pn}|\phi_k\rangle = (PH_0P + V_{\text{eff}}^{pn})|\phi_k\rangle = E_k|\phi_k\rangle \quad , \quad (5)$$

where we require that the eigenfunctions ϕ_k are the projections of the eigenfunctions ψ_k of the ‘‘mother hamiltonian’’

$$|\phi_k\rangle = P|\psi_k\rangle \quad .$$

Then we can express H_{eff}^{pn} formally as

$$H_{\text{eff}}^{pn} = \sum_{k=1}^d E_k|\phi_k\rangle\langle\tilde{\phi}_k| \quad , \quad (6)$$

where the $|\tilde{\phi}_k\rangle$ are the $|\phi_k\rangle$ biorthogonal states satisfying $|\phi_k\rangle\langle\tilde{\phi}_{k'}| = \delta_{kk'}$, and that can be easily obtained using the Schmidt biorthonormalization procedure.

At the end, we can therefore define the effective residual interaction V_{eff}^{pn} as:

$$V_{\text{eff}}^{pn} = \sum_{k=1}^d E_k|\phi_k\rangle\langle\tilde{\phi}_k| - PH_0P \quad . \quad (7)$$

The knowledge of the eigenvalues and eigenfunctions of H^{75} is therefore essential to explicitly derive the effective hamiltonian H_{eff}^{pn} .

It is worth to point out that when solving the H^{75} eigenvalue problem for a A_{val} valence-nucleon system, the corresponding effective hamiltonian H_{eff}^{pn} will contain 1-body, 2-body, ... A_{val} -body contributions. Obviously, the larger is the chosen subspace the smaller is the role of these effective A_{val} -body components.

Since at present, due to the computational complexity, there are no public shell-model codes able to handle these A_{val} -body forces with $n \geq 3$, we have applied the above unitary transformation only to the two valence-nucleon systems (i.e. $^{90}\text{Zr}, ^{90}\text{Sr}, ^{90}\text{Y}$), thus taking into account only TBME of $H_{\text{eff}}^{45}, H_{\text{eff}}^{42}$.

This implies that the energy spectra of $^{90}\text{Zr}, ^{90}\text{Sr}$, and ^{90}Y are exactly the same when diagonalizing $H^{75}, H_{\text{eff}}^{45}$, and H_{eff}^{42} .

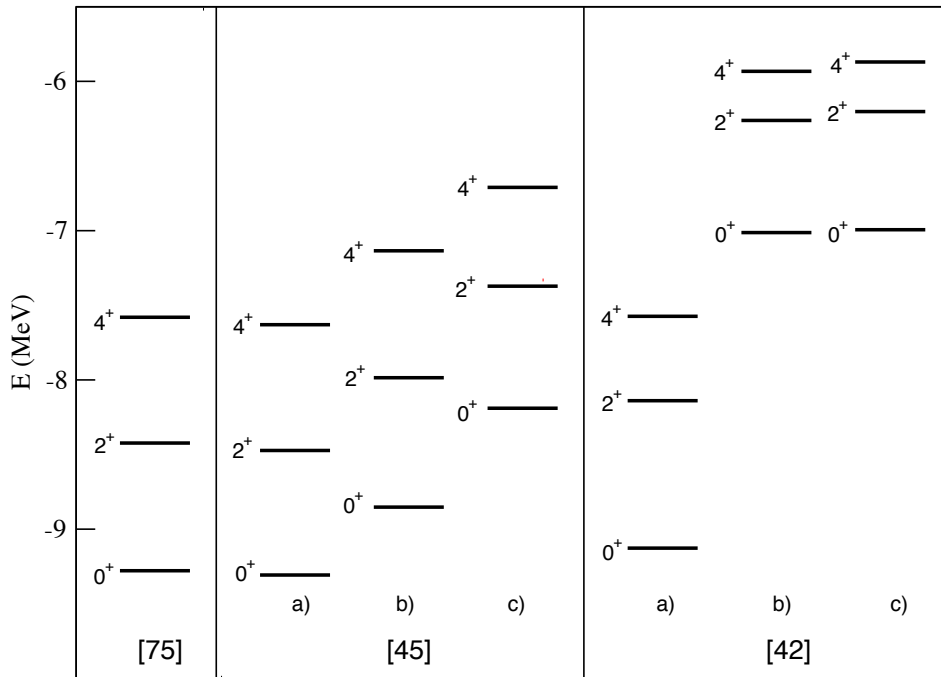


FIG. 3: Yrast $J = 0^+, 2^+, 4^+$ states of ^{96}Mo calculated within model spaces [7, 5], [4, 5], and [4, 2] (see text for details).

To verify the reliability of our truncation scheme, we consider the nucleus ^{96}Mo , which, in our framework, is described as four protons and four neutrons interacting outside ^{88}Sr , and corresponds to the “largest” eigenvalue problem solvable with the “mother” hamiltonian H^{75} for a system with an equal number of valence protons and neutrons.

The shell model calculations with the truncated model spaces [4, 5] and [4, 2] are performed employing:

- the effective hamiltonians H_{eff}^{45} and H_{eff}^{42} ;
- two effective hamiltonians $\tilde{H}_{\text{eff}}^{45}$, $\tilde{H}_{\text{eff}}^{42}$ derived by way of the many-body perturbation theory within the model spaces [4, 5] and [4, 2];
- the hamiltonian H^{75} , but constraining the calculations to model spaces [45], [42].

In Fig. 3 we compare the absolute energies of yrast $J = 0^+, 2^+, 4^+$ states in ^{96}Mo obtained by means of the a), b), c) shell-model calculations. From the inspection of Fig. 2, we expect that the H_{eff}^{42} results will be in a not so good agreement with the H^{75} ones, since there is not a clear separation of the model space P from its complement Q .

It can be noted from Fig. 3 that H_{eff}^{45} is able to reproduce quite well the absolute energies of the “mother hamiltonian” H^{75} , while this is not the case for H_{eff}^{42} . More precisely, even if H_{eff}^{42} reproduces nicely the 2^+ excitation energy, it underestimates the collectivity predicted by the “mother hamiltonian”. As a matter of fact, the $R_{4/2}$ ratio between the calculated excitation energies of the 4^+ versus the 2^+ states, that is equal to 2.0 with H^{75} and H_{eff}^{45} , drops to 1.6 when evaluated with H_{eff}^{42} . For the sake of completeness, it should be observed that the spectra obtained employing the b) and c) hamiltonians are both shifted up with respect to case a), the size of the shift being proportional to the truncation of the model space.

The above results evidence the adequacy of our truncation scheme when the latter is grounded on a neat separation of the model space P from its complement Q , as depicted by the ESPE behavior (see Figs. 1,2).

As mentioned before, we have calculated the $E2$ effective charges consistently with the “mother hamiltonian” H^{75} at the same perturbative order. This means that, when dealing with the effective hamiltonians H_{eff}^{pn} , in order to preserve exactly also the calculated transition rates for the two-valence nucleon systems, the effective $E2$ operator should be further renormalized to take into account the neglected degrees of freedom. In this way, one would obtain an effective two-body $E2$ operator to be employed to calculate the electric quadrupole properties of the systems with a number of valence nucleons greater than two. At our knowledge, however, there’s no public shell-model code able to calculate transition rates driven by two-body transition operators, therefore

we have calculated the $E2$ transition rates using the effective charges derived consistently with H^{75} . As a consequence, the eventual observed discrepancy between the $E2$ properties calculated with H^{75} and those with the effective hamiltonians H_{eff}^{pn} is always a signature of the fact that the corresponding H^{75} wave functions have relevant components outside the truncated $[pn]$ model space.

III. RESULTS

We report the results we have obtained for the even $Z \leq 50$ isotopic chains, namely Zr, Mo, Ru, Pd, Cd, and Sn isotopes with even neutron number. We compare the results obtained using the three different effective hamiltonians H^{75} , H_{eff}^{45} , and H_{eff}^{42} , focusing attention on the quadrupole properties, i.e. yrast 2^+ excitation energies and $B(E2; 0_1^+ \rightarrow 2_1^+)$ transition rates. Calculations have been performed using the public version of the ANTOINE shell-model code [23].

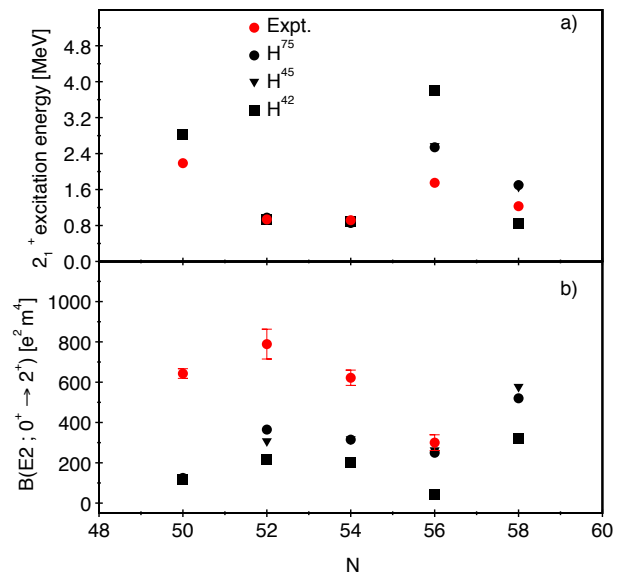


FIG. 4: (Color online) (a) Experimental [36] (red circles) and calculated (black symbols) excitation energies of the yrast $J^\pi = 2^+$ states and (b) $B(E2; 2_1^+ \rightarrow 0_1^+)$ transition rates for zirconium isotopes as a function of N . Circles, triangles, and squares refer to results obtained with H^{75} , H_{eff}^{45} , and H_{eff}^{42} , respectively.

A. Zr isotopes

In our framework Zr isotopes are described as two valence protons and $(N - 50)$ valence neutrons outside ^{88}Sr , therefore ^{90}Zr is a two-valence particle system and by definition, as mentioned in Sec. II, its calculated energy spectrum is exactly preserved by the three effective hamiltonians. This can be seen in Fig. 4 where the cal-

culated excitation energies of the yrast 2^+ states ($E_{2_1^+}^{ex}$) and the $B(E2; 0_1^+ \rightarrow 2_1^+)$ transition rates are reported as a function of N , and compared with the experimental data. The calculated $E_{2_1^+}^{ex}$ are indistinguishable up to $N = 54$, while for $N = 56, 58$ the H_{eff}^{42} eigenvalues are quite different from the H^{75} and H_{eff}^{45} ones, the former predicting a shell closure for $N = 56$.

The discrepancy obtained using H_{eff}^{42} , when evolving the number of neutrons, can be interpreted in terms of the Zr neutron ESPE, whose behavior as a function of N is reported in Fig. 5. The two neutron orbitals $0g_{7/2}$ and $2s_{1/2}$ are very close in energy, so that, when filling the $1d_{5/2}$ orbital, the reduction of the neutron model space to only two orbitals becomes too severe, and H_{eff}^{42} is not able to take into account effectively the neglected $2s_{1/2}$ degrees of freedom.

Similar considerations can be drawn for the electric quadrupole transition rates; the agreement between the H_{eff}^{42} results and the H^{75} and H_{eff}^{45} ones can be considered satisfactory up to $N = 54$, while deteriorating for heavier isotopes.

As regards the comparison with the experiment, the observed behavior of the $E_{2_1^+}^{ex}$ is well reproduced by the H^{75} and H_{eff}^{45} hamiltonians. This is not the case for the $B(E2; 0_1^+ \rightarrow 2_1^+)$ rates, their values being strongly underestimated by the calculations. Our results are not able to describe adequately the quadrupole collectivity that is observed for $N = 50 - 54$.

This may be traced back to the non-negligible role of the $Z = 38$ proton cross-shell excitations, as pointed out in Ref. [37], that should be explicitly included in the calculations.

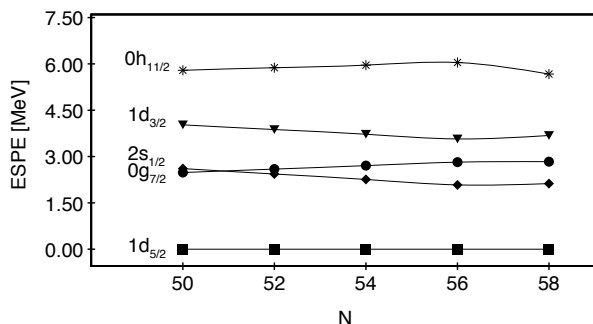


FIG. 5: Zr neutron ESPE calculated from H^{75} as a function of N .

B. Mo isotopes

In Fig. 6 we show the behavior of the calculated $E_{2_1^+}^{ex}$ and $B(E2; 0_1^+ \rightarrow 2_1^+)$ transition rates as a function of N , and compare them with the available experimental data. The results obtained using H^{75} are reported only up to

$N = 54$, since from $N = 56$ on the dimensions of the eigenvalue problem are out of reach for the shell-model code we have employed.

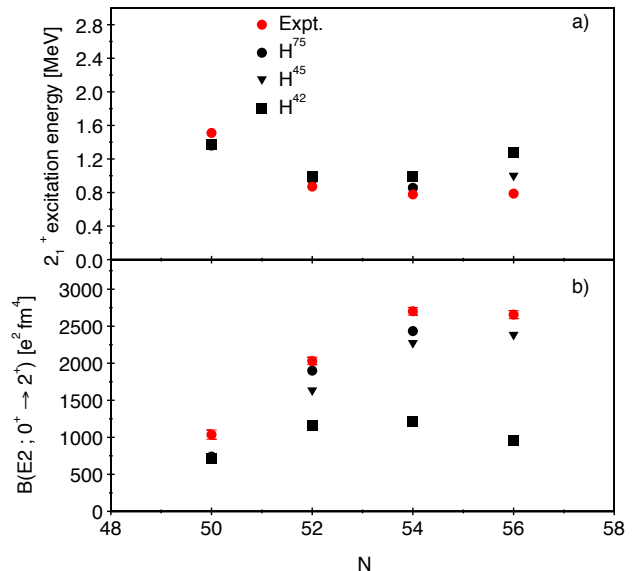


FIG. 6: (Color online) Same as in Fig. 4, for Mo isotopes.

Mo isotopes have four valence protons outside ^{88}Sr , therefore the $0g_{9/2}$ proton orbital begins to be filled, and this induces a relevant collectivity by way of the attractive tensor force acting between the proton $0g_{9/2}$ and the neutron $0g_{7/2}$ orbitals. This implies that the energies are less sensitive to the single-neutron structure and, consequently, a $N = 56$ subshell closure is not expected, even if the neutron ESPE reported in Fig. 7 are similar to those for Zr isotopes. As a matter of fact, while in the ground state (g.s.) wave function of ^{96}Zr the $1d_{5/2}$ neutron orbital is 94% full, its occupation drops to 74% in the ^{98}Mo g.s., owing to the strong interaction $\pi 0g_{9/2} - \nu 0g_{7/2}$. As a consequence, a possible shell closure is obviously prevented, and the reliability of a neutron model-space truncation holds up to $N = 56$, the eigenvalues of the three hamiltonians being very close to each other.

The situation is quite different for the $E2$ transition rates; starting from $N = 52$ the results obtained with H_{eff}^{42} are far from those provided by H^{75} , H_{eff}^{45} , the former transition rates being strongly lower than the latter. The model space spanned only by the $1d_{5/2}$ $0g_{7/2}$ neutron orbitals is clearly not able to describe the onset of quadrupole collectivity, and once again we mention the need to include effective two-body $E2$ operator to cure this deficiency.

In this connection it is worth to stress the reliability of the H_{eff}^{45} hamiltonian, whose results are quite close to the H^{75} ones and in a very satisfactory agreement with the experimental data. In particular, the reproduction of the $E2$ strengths seems to indicate that the increase of the number of protons induces a quenching of the $Z = 38$

proton cross-shell excitations.

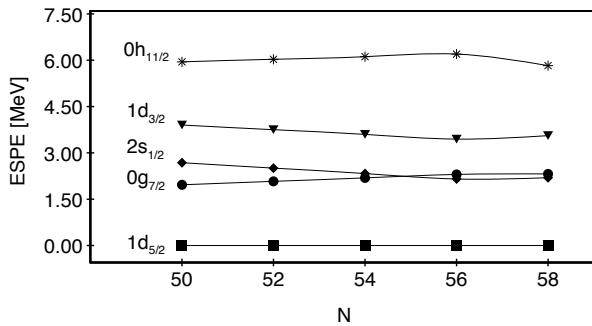


FIG. 7: Same as in Fig. 5, for Mo isotopes.

C. Ru isotopes

The calculated results for ruthenium isotopes are reported and compared with the experimental ones in Fig. 8. Owing to the increase of the valence proton number, we are able to perform calculations with H_{eff}^{45} only up to $N = 54$, so we cannot report a comparison between the different truncation schemes for heavier isotopes.

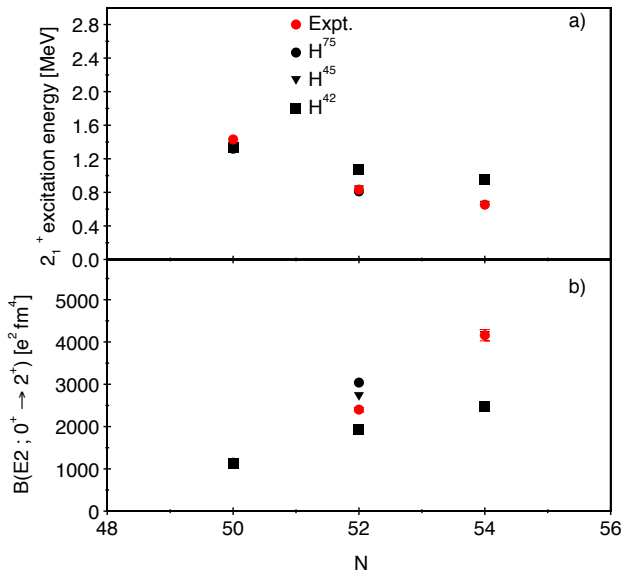


FIG. 8: (Color online) Same as in Fig. 4, for Ru isotopes.

From the inspection of Fig. 8, we see that predicted energies with the three hamiltonians are close and in good agreement with the experiment. Because of the restricted model space, the H_{eff}^{42} hamiltonian - as for Mo isotopes - is not able to describe the quadrupole collectivity as evidenced by the $E2$ transition rates.

The H_{eff}^{45} predicted rates are instead very close to those

of the “mother hamiltonian”, and reproduce nicely the collective behavior.

In Fig. 9 the calculated neutron ESPE of Ru isotopes are reported up to $N = 58$. It can be observed a slight lowering of the $0g_{7/2}$ ESPE, the latter starting to detach from the $1d_{3/2}, 2s_{1/2}$ ones.

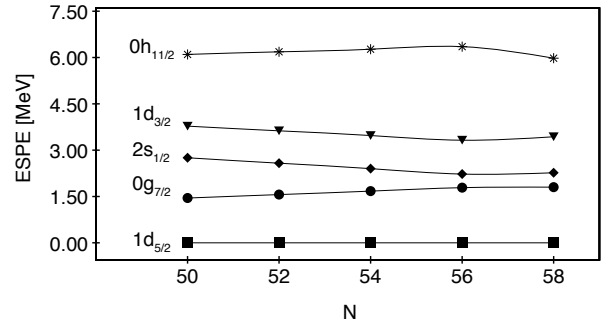


FIG. 9: Same as in Fig. 5, for Ru isotopes.

D. Pd isotopes

From the inspection of Fig. 10, where the neutron ESPE for Pd isotopes are shown as a function of N , it can be seen that the half filling of the proton $g_{9/2}$ orbital has induced a sizeable downshift of the neutron $g_{7/2}$ orbital and the rise of an energy gap ($\simeq 2\text{MeV}$) between the $d_{5/2}$ and $g_{7/2}$ orbitals and the higher ones.

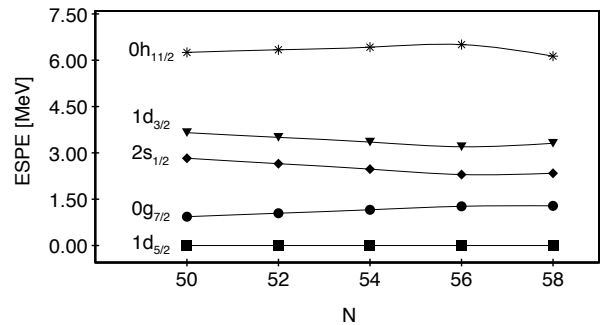


FIG. 10: Same as in Fig. 5, for Pd isotopes.

The calculated eigenvalues are in a good agreement with the data up to $N = 54$ (see Fig. 11), ^{100}Pd being the heaviest computationally attainable isotope with the H_{eff}^{45} hamiltonian, and the observed behavior of the $E_{2_1^+}^{ex}$ is satisfactorily reproduced. The $B(E2; 0_1^+ \rightarrow 2_1^+)$ results with H_{eff}^{45} and H_{eff}^{42} are remarkably different, especially for $N = 54$. This means that the calculated wave functions with H_{eff}^{45} contain relevant neutron components involving the $s_{1/2}, d_{3/2}$ and $h_{11/2}$ orbitals, testifying the need of

an effective two-body $E2$ operator, which will take into account better the neglected neutron degrees of freedom.

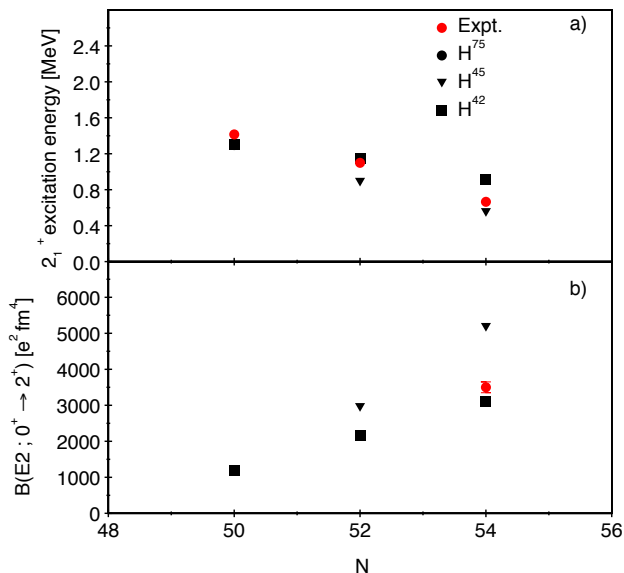


FIG. 11: (Color online) Same as in Fig. 4, for Pd isotopes.

It is worth to note that the comparison with the sole available experimental transition rate shows that the $B(E2)$ s with H_{eff}^{45} overestimate the quadrupole collectivity, at least for $N = 54$.

E. Cd isotopes

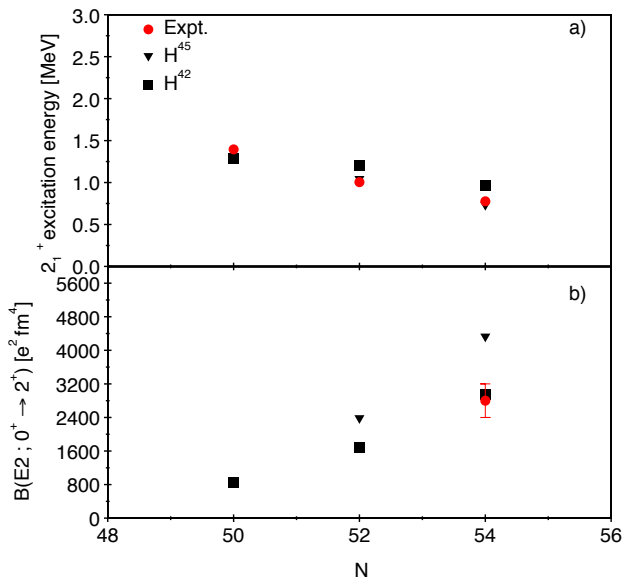


FIG. 12: (Color online) Same as in Fig. 4, for Cd isotopes.

In Figs. 12 and 13 we report, respectively, the calculated $E_{2_1^+}^{ex}$ and $B(E2; 0_1^+ \rightarrow 2_1^+)$ transition rates compared with the experimental ones, and the neutron ESPE.

As it can be seen, almost the same comments made for palladium isotopes still hold for Cd ones. The gap between the $(d_{5/2}, g_{7/2})$ and $(s_{1/2}, d_{3/2}, h_{11/2})$ neutron orbitals increases, due to the progressive filling of the proton $g_{9/2}$ orbital. The H_{eff}^{42} hamiltonian is able to reproduce the eigenvalues of the hamiltonian H_{eff}^{45} , while the lack of relevant components of the wave functions in the subspace spanned by the $s_{1/2}, d_{3/2}, h_{11/2}$ neutron orbitals make the calculated H_{eff}^{42} transition rates for $N = 54$ smaller than the H_{eff}^{45} ones.

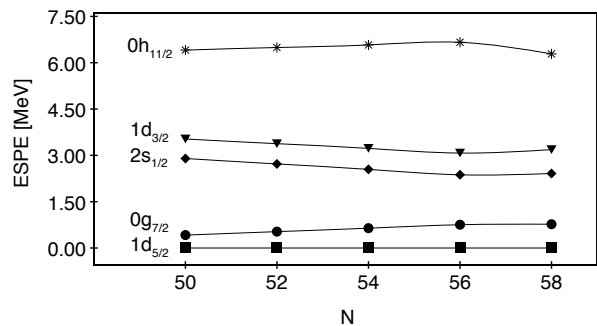


FIG. 13: Same as in Fig. 5, for Cd isotopes.

F. Sn isotopes

The inspection of Fig. 14 evidences that the complete filling of the proton $0g_{9/2}$ orbital induces a 3 MeV energy gap at $Z = 50$ between the $1d_{5/2}, 0g_{7/2}$ subspace and that spanned by the $2s_{1/2}, 1d_{3/2}, 0h_{11/2}$ orbitals.

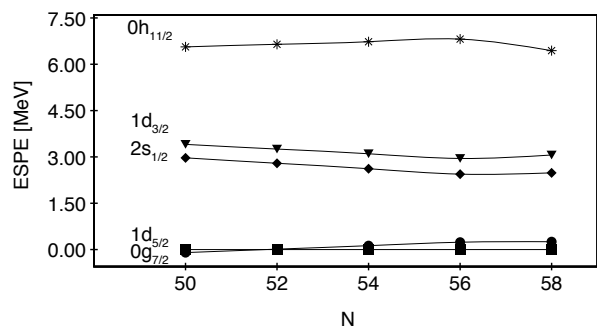


FIG. 14: Same as in Fig. 5, for Sn isotopes.

This, obviously, suddenly enforces the effectiveness of our truncation scheme when using H_{eff}^{42} . As a matter of fact, the quadrupole electric transition rates and the

excitation energies of the yrast 2^+ states calculated with H_{eff}^{42} , reported in Fig. 15, are in good agreement with those obtained with H_{eff}^{45} . Moreover, it can be seen that the calculations with H_{eff}^{42} are able to reproduce quite well the experimental $E_{2_1^+}^{\text{ex}}$ and the $B(E2; 0_1^+ \rightarrow 2_1^+)$ up to $N = 54$ and, consequently, the onset of collectivity from ^{102}Sn on that is driven by the $Z = 50$ cross-shell excitations (see Ref. [26] for a more complete discussion about this point).

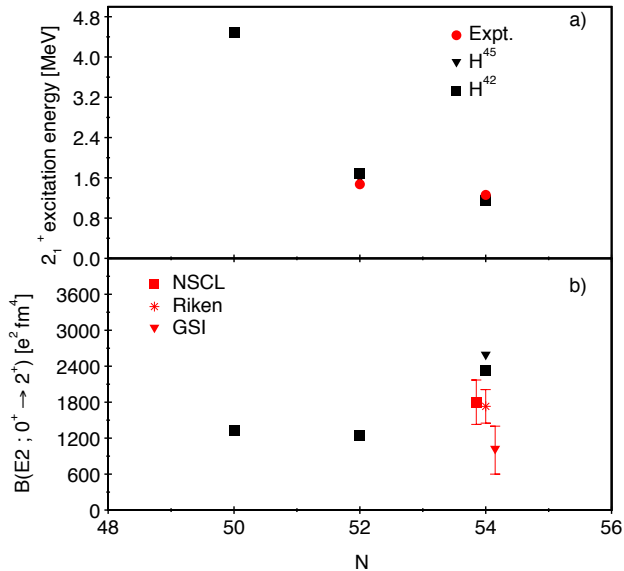


FIG. 15: (Color online) Same as in Fig. 4, for Sn isotopes. The experimental transition strengths for ^{104}Sn are from Refs. [38–40].

Before concluding this subsection, it is in order to point out that the calculations for ^{104}Sn with the H_{eff}^{45} hamiltonian have been performed limiting to 6 the maximum number t of valence particles allowed in the proton $1d_{5/2}, 0g_{7/2}$ and neutron $2s_{1/2}, 1d_{3/2}, 0h_{11/2}$ orbitals, because of the limitations of the ANTOINE shell-model code. To check the reliability of such truncation, we have studied the behavior of the calculated quantities as a function of t . The obtained results are quite stable from $t = 4$ on, the $E_{2_1^+}^{\text{ex}}$ and the $B(E2; 0_1^+ \rightarrow 2_1^+)$ varying less than 1% and 2% respectively, passing from $t = 5$ to $t = 6$.

IV. SUMMARY AND OUTLOOK

The aim of the present paper has been to introduce an original double-step approach to simplify the computational problem of large-scale shell-model calculations. The core of our method is the study of the ESPE of the large-scale hamiltonian, so as to identify the most relevant degrees of freedom to be taken into account in the construction of a truncated shell-model hamiltonian. To this end, a unitary transformation is employed so to derive new effective shell-model hamiltonians defined within a reduced set of single-particle orbitals, accordingly to the ESPE analysis.

We have applied this procedure to a realistic shell-model hamiltonian, whose model space was designed so to describe the $Z = 50$ cross-shell excitations for nuclei outside ^{88}Sr employing seven proton and five neutron orbitals. Because of the behavior of the proton and neutron ESPE, we have identified two new model subspaces made up by four proton orbitals and five and two neutron ones, respectively, and transformed our original hamiltonian in these subsets.

We have performed calculations for Zr, Mo, Ru, Pd, Cd, and Sn isotonic chains to check the reliability of our procedure. The results obtained with the effectively truncated hamiltonians indicates the ability to reproduce eigenvalues and electromagnetic transition rates of the original shell-model hamiltonian, especially when the ESPE provide a neat separation in energy between the new model subspaces and their complement.

This double-step approach may provide a reliable truncation procedure in any large-scale shell-model calculation. As a matter of fact, we are intended to apply it in other regions, as for example to study isotopic and isotonic chains with valence particle outside doubly-magic ^{132}Sn and ^{208}Pb , where the large model spaces leads to critical situations of the computational complexity, when increasing the number of valence nucleons.

We are also studying the possibility to extend this procedure so to truncate shell-model spaces freezing the degrees of freedom of filled nuclear orbitals, as we already experienced in Ref. [41] but within a perturbative derivation of the reduced effective hamiltonians, and to calculate effective two-body electromagnetic operators, consistently with the unitary transformation of the hamiltonian, so to improve also the reproduction of the corresponding transition rates.

-
- [1] E. Caurier, A. P. Zuker, A. Poves, and G. Martínez-Pinedo, *Phys. Rev. C* **50**, 225 (1994).
 [2] M. Honma, T. Mizusaki, and T. Otsuka, *Phys. Rev. Lett.* **77**, 3315 (1996).
 [3] A. Gade, R. V. F. Janssens, T. Baugher, D. Bazin, B. A. Brown, M. P. Carpenter, C. J. Chiara, A. N. Deacon, S. J. Freeman, G. F. Grinyer, et al., *Phys. Rev. C* **81**,

051304 (2010).

- [4] J. Ljungvall, A. Görgen, A. Obertelli, W. Korten, E. Clément, G. de France, A. Bürger, J.-P. Delaroche, A. Dewald, A. Gadea, et al., *Phys. Rev. C* **81**, 061301 (2010).
 [5] T. Baugher, A. Gade, R. V. F. Janssens, S. M. Lenzi, D. Bazin, B. A. Brown, M. P. Carpenter, A. N. Deacon,

- S. J. Freeman, T. Glasmacher, et al., Phys. Rev. C **86**, 011305 (2012).
- [6] H. L. Crawford, R. M. Clark, P. Fallon, A. O. Macchiavelli, T. Baugher, D. Bazin, C. W. Beausang, J. S. Berryman, D. L. Bleuel, C. M. Campbell, et al., Phys. Rev. Lett. **110**, 242701 (2013).
- [7] S. M. Lenzi, F. Nowacki, A. Poves, and K. Sieja, Phys. Rev. C **82**, 054301 (2010).
- [8] K. Sieja, T. R. Rodríguez, K. Kolos, and D. Verney, Phys. Rev. C **88**, 034327 (2013).
- [9] Y. Tsunoda, T. Otsuka, N. Shimizu, M. Honma, and Y. Utsuno, Phys. Rev. C **89**, 031301 (2014).
- [10] T. Togashi, N. Shimizu, Y. Utsuno, T. Otsuka, and M. Honma, Phys. Rev. C **91**, 024320 (2015).
- [11] E. Caurier, F. Nowacki, and A. Poves, Phys. Rev. C **90**, 014302 (2014).
- [12] K. Sieja and F. Nowacki, Phys. Rev. C **81**, 061303 (2010).
- [13] D. Bianco, N. Lo Iudice, F. Andreozzi, A. Porrino, and F. Knapp, Phys. Rev. C **88**, 024303 (2013).
- [14] E. Sahin, M. Doncel, K. Sieja, G. de Angelis, A. Gadea, B. Quintana, A. Görge, V. Modamio, D. Mengoni, J. J. Valiente-Dobón, et al., Phys. Rev. C **91**, 034302 (2015).
- [15] H.-K. Wang, K. Kaneko, and Y. Sun, Phys. Rev. C **91**, 021303 (2015).
- [16] K. Hasegawa, M. Kaneko and S. Tazaki, Nucl. Phys. A **688**, 765 (2001).
- [17] T. Mizusaki and N. Shimizu, Phys. Rev. C **85**, 021301 (2012).
- [18] N. Shimizu, T. Abe, Y. Tsunoda, Y. Utsuno, T. Yoshida, T. Mizusaki, M. Honma, and T. Otsuka, Prog. Theor. Exp. Phys. p. 01A205 (2012).
- [19] C. W. Johnson, W. E. Ormand, and P. G. Krastev, CPC **184**, 2761 (2013).
- [20] E. Caurier, F. Nowacki, and A. Poves, Eur. Phys. J. Web of Conferences **66**, 02106 (2014).
- [21] C. Stumpf, J. Braun, and R. Roth, Phys. Rev. C **93**, 021301 (2016).
- [22] A. Banu, J. Gerl, C. Fahlander, M. Górska, H. Grawe, T. R. Saito, H.-J. Wollersheim, E. Caurier, T. Engeland, A. Gniady, et al., Phys. Rev. C **72**, 061305 (2005).
- [23] E. Caurier, G. Martínez-Pinedo, F. Nowacki, A. Poves, and A. P. Zuker, Rev. Mod. Phys. **77**, 427 (2005).
- [24] A. P. Zuker, J. Retamosa, A. Poves, and E. Caurier, Phys. Rev. C **52**, R1741 (1995).
- [25] E. Caurier and G. Martínez-Pinedo, Nucl. Phys. A **704**, 60c (2002).
- [26] L. Coraggio, A. Covello, A. Gargano, N. Itaco, and T. T. S. Kuo, Phys. Rev. C **91**, 041301 (2015).
- [27] R. Machleidt, Phys. Rev. C **63**, 024001 (2001).
- [28] S. Bogner, T. T. S. Kuo, L. Coraggio, A. Covello, and N. Itaco, Phys. Rev. C **65**, 051301(R) (2002).
- [29] T. T. S. Kuo, S. Y. Lee, and K. F. Ratcliff, Nucl. Phys. A **176**, 65 (1971).
- [30] L. Coraggio, A. Covello, A. Gargano, N. Itaco, and T. T. S. Kuo, Prog. Part. Nucl. Phys. **62**, 135 (2009).
- [31] See Supplemental material at [URL will be inserted by publisher] for the list of two-body matrix elements of the shell-model hamiltonians H_{eff}^{45} and H_{eff}^{42} .
- [32] S. Bogner, T. T. S. Kuo, and L. Coraggio, Nucl. Phys. A **684**, 432c (2001).
- [33] L. Coraggio, A. Covello, A. Gargano, N. Itaco, and T. T. S. Kuo, Ann. Phys. **327**, 2125 (2012).
- [34] K. Suzuki and S. Y. Lee, Prog. Theor. Phys. **64**, 2091 (1980).
- [35] T. Otsuka, T. Suzuki, R. Fujimoto, H. Grawe, and Y. Akaishi, Phys. Rev. Lett. **95**, 232502 (2005).
- [36] Data extracted using the NNDC On-line Data Service from the ENSDF database, file revised as of February 3, 2016.
- [37] K. Sieja, F. Nowacki, K. Langanke, and G. Martínez-Pinedo, Phys. Rev. C **79**, 064310 (2009).
- [38] G. Guastalla, D. D. DiJulio, M. Górska, J. Cederkäll, P. Boutachkov, P. Golubev, S. Pietri, H. Grawe, F. Nowacki, K. Sieja, et al., Phys. Rev. Lett. **110**, 172501 (2013).
- [39] V. M. Bader, A. Gade, D. Weisshaar, B. A. Brown, T. Baugher, D. Bazin, J. S. Berryman, A. Ekström, M. Hjorth-Jensen, S. R. Stroberg, et al., Phys. Rev. C **88**, 051301 (2013).
- [40] P. Doornenbal, S. Takeuchi, N. Aoi, M. Matsushita, A. Obertelli, D. Steppenbeck, H. Wang, L. Audirac, H. Baba, P. Bednarczyk, et al., Phys. Rev. C **90**, 061302 (2014).
- [41] L. Coraggio, A. Covello, A. Gargano, and N. Itaco, Phys. Rev. C **89**, 024319 (2014).